ORIGINAL PAPER

Imaging and determining friction forces of specific interactions between human IgG and rat anti-human IgG

Zhengjian Lv · Jianhua Wang ·
Guoping Chen · Linhong Deng

Abstract Covalently immobilized rat anti-human immunoglobulin (IgG) monolayers on thiol-modified gold substrates and human IgG linked with the tips were fabricated using the self-assembled monolayer method, and interactions between these systems were studied by friction force microscopy (FFM). In addition to observation of distinct nanostructures of protein monolayers due to recognition events, FFM also quantified the friction force due to protein–protein-specific interactions. The average friction force due to interactions between the antigen functionalized tip and the antibody monolayer was determined as 200–250 pN, significantly greater than that between either the bare tip and the antibody monolayer (0–50 pN), or the blocked antigen tip and the antibody monolayer (50–100 pN), indicative of antigen/antibody-specific interactions. These results, taken together, suggest that FFM is not only capable of tracking recognition events, but also quantifying the friction force due to specific interactions between biological molecules, such as antigen and antibody.

Keywords Human IgG · Rat anti-human IgG · Self-assembled monolayer · Friction force microscopy

1 Introduction

Many biological functions are known to be regulated or mediated by antibody-based protein–protein interactions (PPIs) [1–3], and thus probing and characterizing these inter-actions has become increasingly important in the development of novel drugs and medical diagnostics [4–7]. So far, a number of methods have been developed for investigating PPIs, including surface force apparatus [8], surface plasmon resonance (SPR) [9], and atomic

Z. Lv · J. Wang (✉) · G. Chen · L. Deng (✉)
Key Laboratory of Biorheological Science and Technology, Ministry of Education, and
Institute of Biochemistry and Biophysics, College of Bioengineering,
Chongqing University, Chongqing, 400044, China
e-mail: wjh@cqu.edu.cn, denglh@cqu.edu.cn

 Springer

force microscopy (AFM) [10]. Among these methods, AFM has emerged as the most widely used one because of its high spatial resolution, high force sensitivity, and capability of measuring in near physiological environment and without special sample preparation [11].

To measure PPIs in contact-mode AFM, the cantilever tip can be moved in a direction either perpendicular or parallel to the surface of the stationary substrate as illustrated in Fig. 1a. When pulling the tip perpendicularly away from the substrate, the protein interactions between the tip and the substrate exert a rupture force that causes a vertical deflection of the cantilever until the protein binding ruptures, which can be measured and converted into the magnitude of the rupture force (Fig. 1a upper panel). In contrast, when moving the tip across the substrate for a lateral unbinding, the protein interactions between the tip and the substrate act like a friction force that causes a torsional bending of the

Fig. 1 Scheme of measurements of rupture and friction forces between antigen and antibody (a). The *top panel* shows the principle of rupture force microscopy and an ideal rupture force-distance curve, while the *bottom panel* represents friction force microscopy and an ideal friction loop, and a typical frictional loop recorded by FFM (CSPM 5000) (b): at a given scan line, the tip advances the surface of the monolayer and retracts. As the cycle is completed, a friction loop is recorded accordingly. The friction loop is circular closed curve with symmetry, which allows the voltage change ΔV to be monitored. The ΔV can be converted into friction forces, thus reflecting the frictional behavior of the measured surfaces
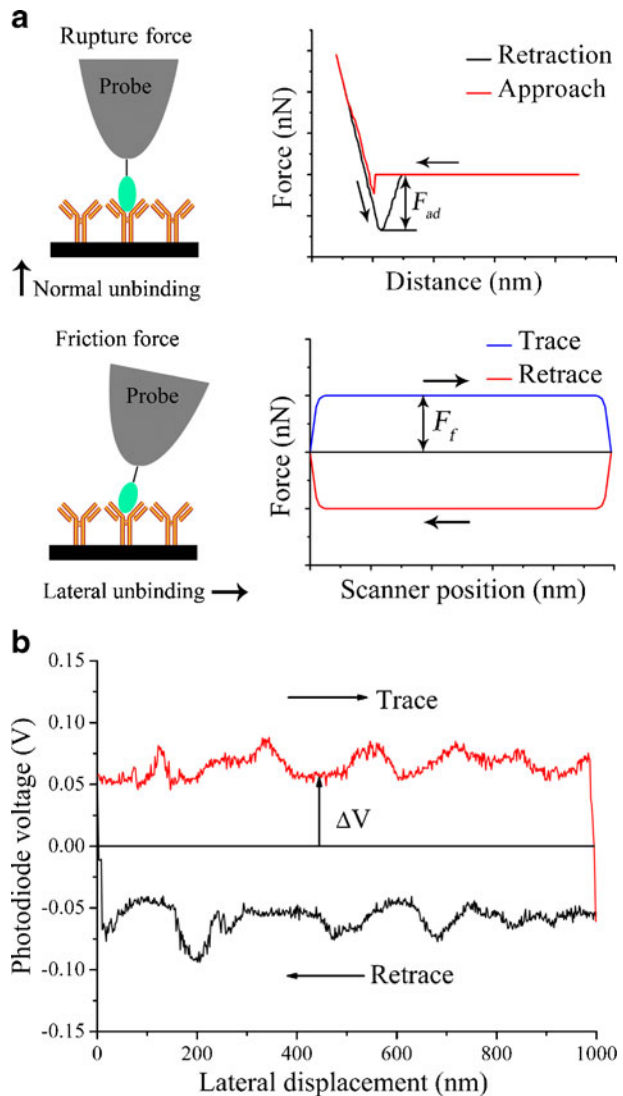
cantilever, which can then be measured and converted into the magnitude of the friction force (Fig. 1a lower panel), an operation also known as the friction force microscopy (FFM) [12].

Previous studies have shown that FFM could provide quantitative information of both chemical composition and molecular pattern of a material's surface [13], especially when subtle variations occur [14], with good reproducibility [15]. However, as compared with probing rupture forces [16, 17] or probing friction forces, FFM has been much less studied, despite its potential as an alternative technique for elucidating biological systems [18, 19].

The motivation of this study was to evaluate whether, by analyzing the friction force images and the friction responses from different experimental systems, FFM can be applied to detect specific interactions between antigen and antibody. Human IgG and rat anti-human IgG were used as a model biological system, and friction force images and friction forces between different tips and samples were obtained by FFM using the tip and the substrate without or with protein coating. The results suggest that FFM may provide a reliable tool for probing specific interactions between biological molecules.

2 Materials and methods

To investigate PPIs through FFM, the protein molecules must be prepared onto the surface of the substrate, and the AFM tip (a process known as functionalizing AFM tip or tip chemistry). Thus, we used a thiol-based self-assembled monolayer (SAM) for protein immobilization because of its effectiveness and simplicity [20, 21]. The details of sample preparation, FFM imaging and friction force measurement are described as follows.

2.1 Gold-coated substrates

Gold-coated substrates were prepared by vapor deposition of gold onto freshly cleaved mica in a high vacuum evaporator at $\sim 10^{-7}$ Torr. Mica substrates were preheated to 325°C for 2 h by a radiator heater before deposition. Evaporation rates were 0.1–0.3 nm/s, and the final thickness of the gold films was $\sim$200 nm. A chromium layer was also vapor-deposited and sandwiched between the gold and mica to strengthen the adhesion between the surfaces. The gold-coated substrate was then annealed in H_2 flame for 1 min before use.

2.2 SAM of thiols on gold surface

The preparation of the protein monolayer was performed as formerly reported [22], and the process is described below. The bare gold-coated substrate prepared as above was thoroughly cleaned in hot piranha solution (v/v H_2SO_4:H_2O_2 =3:1) for 30 min. The cleaning process was carried out with extreme care because piranha solution is highly reactive and may explode when in contact with organic solvents. The gold-coated substrate was then immersed into the ethanol solution of 1 mM 16-mercaptohexadecanoic acid (MHA) for 24 h to produce the thiol-based SAM on the gold surface, and unbound thiols were removed by ultrasonication in pure ethanol for 2 min. The prepared SAM was then rinsed sequentially with pure ethanol, ultra-pure water, and finally dried in a N_2 stream before use.

2.3 Protein immobilization onto the MHA-modified gold substrate

Protein immobilization to SAM was carried out as described before with minor modification [23]. In brief, the thiol-based SAM was treated in the solution of 2 mg/ml

N-hydroxysulfosuccinimide (NHS) and 2 mg/ml 1-ethyl-3-(dimethylaminopropyl) carbodi-imide hydrochloride (EDC) in PBS for 1 h, which activated the carboxylic acid terminal groups of the SAM. After thorough rinsing with ultra-pure water, and drying in a N_2 stream, the activated SAM was then immersed into the protein solution of 7 µg/ml rat anti-human IgG in PBS and incubated at 4°C for 8 h to immobilize the proteins onto the MHA film. The prepared sample of the protein layer was stored in PBS at 4°C before use.

2.4 Chemistry for FFM tip

The process of tip chemistry is very similar to that of protein immobilization. First, the tip was cleaned in piranha solution for 30 min and washed with ultra-pure water, then modified with 1 mM MHA through a self-assembly method. The SAM-modified tips were activated by EDC and NHS in PBS buffer solution and then incubated in 10 µg/ml human IgG PBS solution at 4°C for 6 h. Finally, the specimens were stored in PBS solution at 4°C. Notably, if not specified, the tips used in this study were bare tips without modification.

2.5 FFM imaging

All images were acquired using Benyuan CSPM 5000 scanning probe microscope (Benyuan Co., China) equipped with a 26-µm E scanner. Commercially available gold-coated Si_3N_4 cantilever tips (BudgetSensors®, Innovative Solutions Bulgaria Ltd., Bulgaria) were used. All FFM images were taken in PBS buffer solution with typical scanning rate of 2.0 Hz. The scanning scopes were all set at 2×2 µm to better compare the friction force images of different surfaces. The friction force images of the bare gold, and the antibody monolayer treated without or with free antigen were recorded. Moreover, the antigen-antibody recognition profiles of were obtained by using antigen-functionalized AFM tips scanning over the antibody monolayer. All FFM images were uniformly set at 512×512 pixels. With regard to obtained images, difference in brightness arose from the differences in interactions.

2.6 Specificity of the recognition events

Identification of recognition events only requires that any nonspecific interaction force between human IgG and rat anti-human IgG be measured and excluded. This was done by a blocking experiment performed as follows. First, the AFM tip functionalized with human IgG was incubated for 30 min in a solution of rat anti-human IgG to block the binding sites of the antigen on the tip. Then, the nonspecific interaction force was obtained by the same imaging as described above, but performed using the blocked tip.

2.7 Measurements of friction force between antigen and antibody

In our FFM experiments, the friction force was calibrated by a previously reported nondestructive and fast method. For details of the calibration, please refer to literature [24, 25].

In the present study, rectangular cantilevers were used for force measurement as suggested by Sader [26]. The rupture and friction force was measured, respectively, as [24]:

$$F_n = c_n z \tag{1}$$

and

$$F_f = \frac{3}{2} c_t \frac{h}{l} S\Delta U \tag{2}$$

where z is the vertical deflection of the cantilever, S is the sensitivity of the photodetector in units of nanometers per volt. ΔU is the change in voltage, $c_n = \frac{Ewt^3}{4l^3}$ and $c_t = \frac{Gwt^3}{3lh^2}$ are the normal and lateral spring constants of the rectangular shaped cantilever of length l, width w, height h, Young's modulus E, shear modulus G (72.5 GPa) [24], and $t = \beta f_0 l^2$ with a material constant $\beta = 7.23 \times 10^{-4}$ s/m determined by measuring the resonance frequency f_0 of the unloaded cantilever [24, 26, 27]. The normal and lateral cantilever spring constants of the AFM tips were determined to be $0.05 \sim 0.08$ N/m and $14.86 \sim 16.35$ N/m, respectively.

In friction force operation, the cantilever is usually tilted at an angle between 10–15° with respect to the surface to ensure that the tip apex first contacts the substrate when the tip approaches. Thus, a factor $\cos \alpha$ has to be taken into account for the calibration process [27]. In our FFM system, the tilt angle α was found to be 12° and corrected correspondingly in the friction force calculation.

FFM force measurements were all taken in PBS buffer solution using a Benyuan CSPM 5000 scanning probe microscope. Frictional loops were obtained for sliding velocity of 30 μm/s with applied loads of up to 2.5 nN, and the temperature was controlled at 25°C. Additionally, the force–displacement curves were obtained at each setpoint voltage for the vertical deflection of the cantilever to determine the normal load applied to the sample, and the calculation of F_n was thus carried out as previously performed [28].

2.8 Materials

MHA, EDC, and NHS were purchased from Sigma Aldrich Chemical Co. and used as received. Phosphate-buffered saline (PBS, 140 mM NaCl, 3 mM KCl, pH 7.4) and ethanol (guaranteed grade) were purchased from Merck Co., and ultra-pure water (resistivity of 18.2 MΩ cm) was obtained by a Millipore purification system. Human IgG and rat anti-human IgG were purchased from Biosun Co. (China).

3 Results and discussion

3.1 Recognition events between antigen and antibody monitored by FFM

The friction force images of the bare gold, and the antibody monolayers treated without or with free antigen are shown in Fig. 2a, b and c, respectively. All obtained surfaces show good uniformity. More specifically, the bare gold shows flat and island-like structures (Fig. 2a) with average size (diameter) of 33.85 ± 2.76 nm, whereas the antibody monolayer shows spherical structures (Fig. 2b) with typical size of 54.16 ± 5.42 nm. However, after treatment with free antigen, the surface of the antibody monolayer (Fig. 2c) shows rock-like structures, and the size of the structures increases from 54.16 ± 5.42 to 96.77 ± 10.35 nm; the size of the observed particles is almost double that of the antibody molecule itself, indicating that specific interactions existed and the antigen–antibody complexes were formed. Furthermore, the recognition profiles of antigen–antibody recognition profiles were recorded using antigen-functionalized tips as a substitute for bare tips (Fig. 2d). Comparing to the antibody monolayer (Fig. 2b), the recognition profiles show significant surface
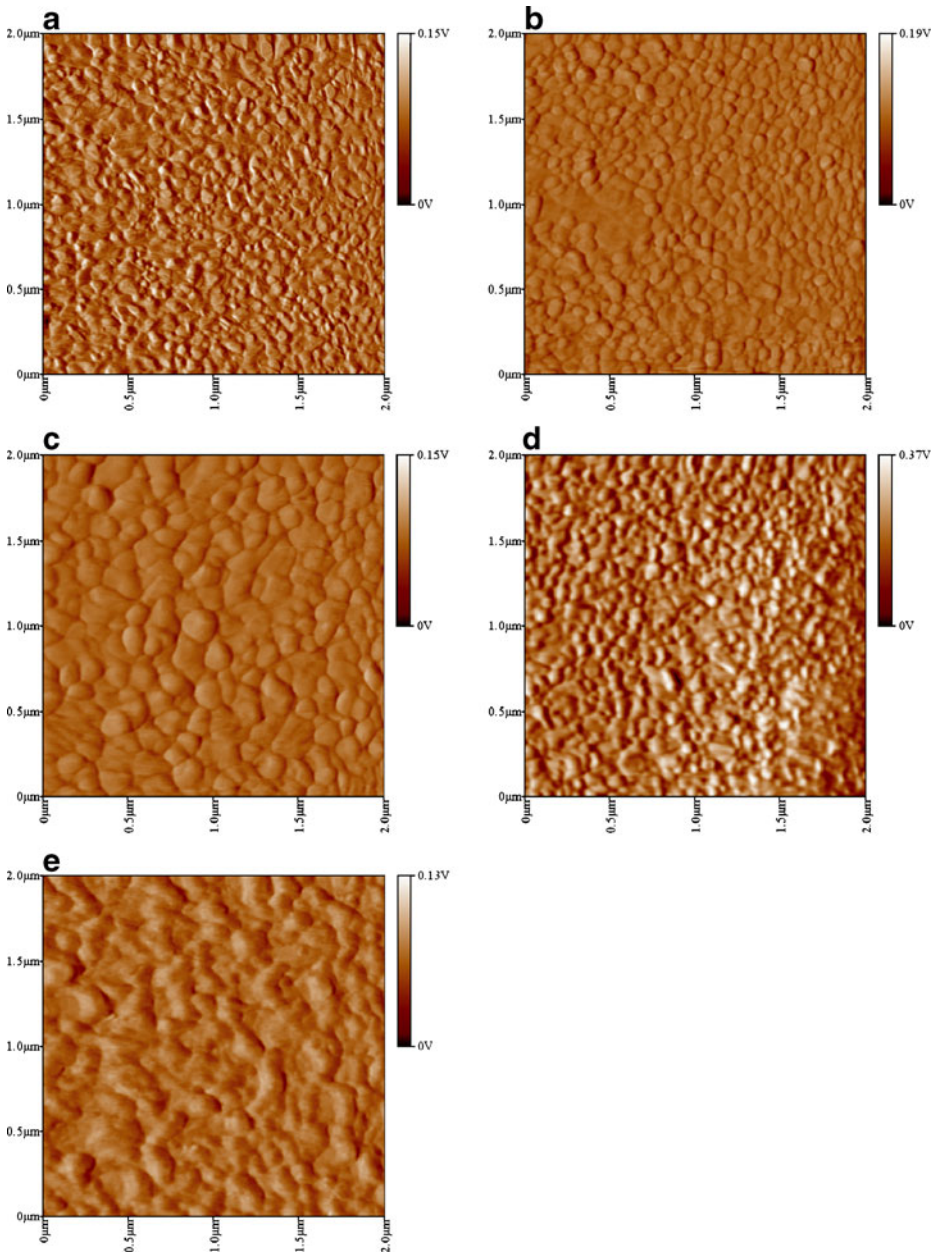
Fig. 2 Friction force images of different surfaces recorded by FFM. They are the bare gold substrate (**a**), the rat anti-human IgG monolayers treated without (**b**) or with free antigen (**c**), recognition profiles of antigen–antibody by replacing the bare tips with antigen-functionalized tips (**d**), and the blocking experiment by masking the binding sites of the antigen molecules which were immobilized onto the AFM tips (**e**), respectively. All FFM imaging was performed in PBS buffer solution with a scanning size of $2 \times 2 \ \mu m^2$

deformation and irregular structures. Such phenomena may be caused by the specific interactions between antigen and antibody, which initiate the torsional bending of the tip and affect the stretching of antibody molecules [19], finally giving rise to large unbinding forces. These recognition profiles suggest that there are specific interactions between the antigen-tethered tip and the antibody monolayer, and the unbinding forces lead to the deformation of the antibody monolayer.

The blocking experiment was also conducted to test the specificity of interactions between antigen and antibody by masking the antigen-binding sites. The plateau-like surface of the blocking experiment was observed (Fig. 2e). This unique friction force image is mainly caused by the large tip radii of the antibody/antigen complex modified tip; when such modified tip scanned over the antibody monolayer, a broadening effect would significantly be introduced, thus introducing an artifact [22, 29]. The real frictional topography of the nanostructures would be obscured due to the existence of the tip broadening effect, and the final observed structures would have much larger sizes than the real sizes.

3.2 Friction force between antigen and antibody determined by FFM

When a relative slide occurs over two contact surfaces, all contact points will be destroyed by shear mode. The clash between the protrusions of the two surfaces will result in rupture and wear, thus preventing movement. The force needed for relative slide which must overcome the shear force is the so-called friction force. There are several models related describing contact mechanics; for example, in a macroscopic situation, Amontons' law,

$$F_f = \mu F_n + F_0, \tag{3}$$

applies, where μ is the kinetic friction coefficient, F_n is the applied normal force, and F_0 is the "residual force", which is related to the adhesion between contacting surfaces [30]. However, from a microscopic point of view, F_f and F_n are not expected to be linear for a single asperity contact, several models can be applied in this case. These models include the Hertzian model, the Derjaguin, Muller, and Toporov model [31], and the Johnson, Kendall, and Roberts (JKR) model [32]. The JKR model incorporates the adhesive force between the tip and the sample. It is applicable to soft materials that experience short-range interactions.

In this study, the relationship between F_f and F_n was investigated; the results are shown in Fig. 3. A linear relationship (line 3, colored in green) between F_f and F_n was observed, with a slope value calculated to be 74.33 ± 2.77 ($R = 0.9013$), in agreement with Amontons' law which states that F_f is directly proportional to F_n, with a constant of proportionality (the so-called friction coefficient) [33]. However, a corner ($F_n = 2.5$ nN) was observed which separates the data into two groups (lines 1 and 2 are linear fits, and are colored in blue and red, respectively); the slope values of lines 1 and 2 were calculated to be 95.97 ± 3.39 ($R = 0.9356$) and 19.91 ± 18.71 ($R = 0.1474$), respectively. Theoretically, deviation from the anticipated linearity might come from multiple asperity contacts or because of plastic deformation of the samples. Some researchers supported the latter notion [34], whereas the others suggested the viscoelastic deformation of samples [35]. However, the deformation of the monolayer, comprising comparatively soft protein molecules on substrate, is significantly more complex from a theoretical perspective. In the present case, this discrepancy may stem from the transition of protein conformation, in which the antigen and antibody adjust themselves to the most optimal binding conformations. When F_n was larger than 2.5 nN, the tip would squeeze the antibody monolayer, causing friction
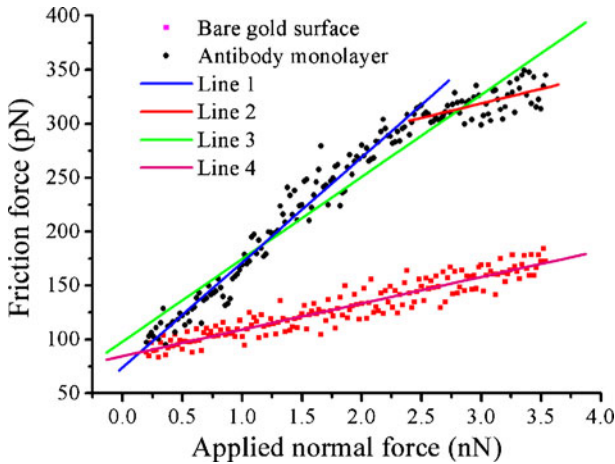
Fig. 3 Plot of applied normal force versus friction force for the human IgG modified tip/rat anti-human IgG monolayer system ($n = 168$, upper group, *colored in black*). The linear fit is shown in *line 3* which is *colored in green*. A corner ($F_n = 2.5$ nN) is observed which separates the data into two groups, of which the linear fits are shown in *line 1* (*colored in blue*) and *line 2* (*colored in red*), respectively. The slope values of *lines 1, 2*, and *3* were calculated to be 95.97 ± 3.39 ($R = 0.9356$), 19.91 ± 18.71 ($R = 0.1474$) and 74.33 ± 2.77 ($R = 0.9013$), respectively. In addition, the relationship between antigen-functionalized tip and bare gold surface is presented in *line 4* (lower group, *colored in magenta*), of which the slope was counted to be 24.45 ± 0.69

scattering. Moreover, to better interpret the relationship between the friction force and the applied normal force for the antibody monolayer, data for the gold surface are also presented in Fig. 3 (square dots). The slope of the linear fit was calculated to be 24.45 ± 0.69 (line 4), which is significantly lower than that of the antigen–antibody system, indicating that the antibody monolayer has a rougher surface and that the frictional force is larger in the presence of antigen.

In addition, at a given F_n, the frictional behavior of these three different systems were also investigated. The different friction force distributions of the bare tip/antibody system, the blocking experiment, and the antigen/antibody system were determined and represented by black, red, and blue bars in Fig. 4, respectively. In particular, the friction force of the bare tip/antibody system was determined to be lower than 50 pN (Fig. 4, black bar), which was used as a reference. However, the friction force between antigen and antibody was calculated to be 200–250 pN (Fig. 4, blue bar), which is slightly higher than that of concanavalin A/carboxypeptidase Y system [19], but significantly lower than that of the thiol–thiol system [36]. The value of F_f may be influenced by several factors: (1) chain length (the longer the chains, the greater the cohesive interactions between chains, longer chains of thiols, stabilized by Van der Waals (vdW) attractions form more compact and rigid layers [34]); (2) sliding velocity [37]; (3) temperature, (the influence of temperature on nanotribology is not well understood yet [38]); (4) F_n; and (5) interfacial surface energy [14].

Moreover, the friction force of the blocking experiment was determined to be 50–150 pN (Fig. 4, blue bar); this value was expected because the modified tip used in the blocking experiment has a rougher surface and larger real contact area than that of the bare tip, thus giving rise to a moderate-to-large friction force. The experimental value of 50–
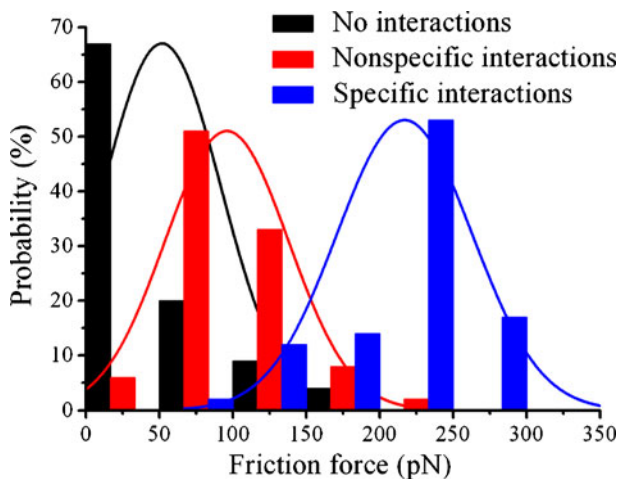
Fig. 4 Histogram of distributions of all measured friction forces. The friction forces measured when there were no interactions (between the bare tip and the antibody monolayer), only non-specific interactions (the blocking experiment), and specific interactions (between the antigen functionalized tip and the antibody monolayer), were represented by *black*, *red*, and *blue bars*, respectively. The typical friction forces of the bare tip/antibody system, the blocking experiment, and the antigen/antibody system were calculated to be 0–50 pN, 50–150 pN, and 200–250 pN, respectively. The *solid lines* are theoretical Gaussian fits

150 pN is in agreement with the theoretical prediction, which is higher than that of the bare tip/antibody system but lower than that of the blocking experiment. The comparison of friction forces among these systems implies there may be specific interactions for the antigen/antibody system, no specific interactions for the bare tip/antibody system, and non-specific interactions existing when the antigen-binding sites were blocked. Taken together, it is difficult to define the frictional behavior of PPIs at nanoscale, in such a case study. Despite this, the friction force measurements still allow to qualitatively demonstrate the specific interactions between antibody and antigen.

4 Conclusions

In this work, we used FFM-recorded friction force images and friction forces to investigate interactions between monolayers of rat anti-human IgG (antibody) and human IgG (antigen). The monolayer of rat anti-human IgG or human IgG was covalently immobilized on thiols modified with either gold substrate or an AFM cantilever tip surface, respectively, using the SAM method. The FFM-recorded friction force images displayed distinct nanostructures when the antibody monolayer was scanned by tips of different surface chemistry, demonstrating the ability of FFM to sense specific interactions between antigen and antibody. More importantly, the friction force quantified by FFM also characterized clear differences of interactions between different preparations of the antigen and the antibody monolayers, resulting in an average friction force of 200–250 pN between the antibody monolayer and the antigen-covered tip, 50–150 pN between the antibody monolayer and blocked antigen-covered tip, and 0–50 pN between the antibody monolayer and the bare tip. The large friction force detected between the antigen and the antibody monolayer confirmed the specific interactions between the antigen and the antibody. Altogether, these

results suggest that FFM technique is suitable and reliable for studying specific interactions between biological molecules such as antigens and antibodies.

References

 1. Kwong, P.D., Wyatt, R., Robinson, J., Sweet, R.W., Sodroski, J., Hendrickson, W.A.: Structure of an HIV gp120 envelope glycoprotein in complex with the CD4 receptor and a neutralizing human antibody. Nature **393**, 648–659 (1998)
 2. Calarese, D.A., Scanlan, C.N., Zwick, M.B., Deechongkit, S., Mimura, Y., Kunert, R., Zhu, P., Wormald, M.R., Stanfield, R.L., Roux, K.H., Kelly, J.W., Rudd, P.M., Dwek, R.A., Katinger, H., Burton, D.R., Wilson, I.A.: Antibody domain exchange is an immunological solution to carbohydrate cluster recognition. Science **300**, 2065–2071 (2003)
 3. Carroll, M.C.: The complement system in regulation of adaptive immunity. Nat. Immunol. **5**, 981–986 (2004)
 4. Peretz, D., Williamson, R.A., Kaneko, K., Vergara, J., Leclerc, E., Schmitt-Ulms, G., Mehlhorn, I.R., Legname, G., Wormald, M.R., Rudd, P.M., Dwek, R.A., Burton, D.R., Prusiner, S.B.: Antibodies inhibit prion propagation and clear cell cultures of prion infectivity. Nature **412**, 739–743 (2001)
 5. Li, H., Sethuraman, N., Stadheim, T.A., Zha, D., Prinz, B., Ballew, N., Bobrowicz, P., Choi, B.K., Cook, W.J., Cukan, M., Houston-Cummings, N.R., Davidson, R., Gong, B., Hamilton, S.R., Hoopes, J.P., Jiang, Y., Kim, N., Mansfield, R., Nett, J.H., Rios, S., Strawbridge, R., Wildt, S., Gerngross, T.U.: Optimization of humanized IgGs in glycoengineered Pichia pastoris. Nat. Biotechnol. **24**, 210–215 (2006)
 6. Zhu, H., Bilgin, M., Snyder, M.: Proteomics. Annu. Rev. Biochem. **72**, 783–812 (2003)
 7. Kusnezow, W., Jacob, A., Walijew, A., Diehl, F., Hoheisel, J.D.: Antibody microarrays: an evaluation of production parameters. Proteomics **3**, 254–264 (2003)
 8. Sheth, S.R., Leckband, D.: Measurements of attractive forces between proteins and end-grafted poly(ethylene glycol) chains. Proc. Natl. Acad. Sci. U.S.A. **94**, 8399–8404 (1997)
 9. Karisson, R., Falt, A.: Experimental design for kinetic analysis of protein–protein interactions with surface plasmon resonance biosensors. J. Immunol. Methods **200**, 121–133 (1997)
10. Lin, S., Chen, J.L., Huang, L.S., Li, H.W.: Measurements of the forces in protein interactions with atomic force microscopy. Curr. Proteomics. **2**, 55–81 (2005)
11. Fotiadis, D., Scheuring, S., Muller, S.A., Engel, A., Muller, D.J.: Imaging and manipulation of biological structures with the AFM. Micron **33**, 385–397 (2002)
12. Leggett, G.J., Brewer, N.J., Chonga, K.S.L.: Friction force microscopy: towards quantitative analysis of molecular organisation with nanometre spatial resolution. Phys. Chem. Chem. Phys. **7**, 1107–1120 (2005)
13. Colburn, T.J., Leggett, G.J.: Influence of solvent environment and tip chemistry on the contact mechanics of tip-sample interactions in friction force microscopy of self-assembled monolayers of mercaptoundecanoic acid and dodecanethiol. Langmuir **23**, 4959–4964 (2007)
14. Leggett, G.J.: Friction force microscopy of self-assembled monolayers: probing molecular organisation at the nanometre scale. Anal. Chim. Acta. **479**, 17–38 (2003)
15. Ahimou, F., Semmens, M.J., Novak, P.J., Haugstad, G.: Biofilm cohesiveness measurement using a novel atomic force microscopy methodology. Appl. Environ. Microbiol. **73**, 2897–2904 (2007)
16. Lo, Y.S., Zhu, Y.J., Beebe, T.P.: Loading-rate dependence of individual ligand-receptor bond-rupture forces studied by atomic force microscopy. Langmuir **17**, 3741–3748 (2001)
17. Florin, E.L., Moy, V.T., Gaub, H.E.: Adhesion forces between individual ligand–receptor pairs. Science **264**, 415–417 (1994)
18. Choi, J.W., Park, S.J., Nam, Y.S., Lee, W.H., Fujihira, M.: Molecular pattern formation using chemically modified cytochrome. Colloids Surf. B, Biointerfaces **23**, 295–303 (2002)
19. Lekka, M., Kulik, A.J., Jeney, S., Raczkowska, J., Lekki, J., Budkowski, A., Forro, L.: Friction force microscopy as an alternative method to probe molecular interactions. J. Chem. Phys. **123**, 014702 (2005)

20. Ferretti, S., Paynter, S., Russell, D.A., Sapsford, K.E., Richardson, D.J.: Self-assembled monolayers: a versatile tool for the formulation of bio-surfaces. Trends. Analyt. Chem. **19**, 530–540 (2000)
21. Love, J.C., Estroff, L.A., Kriebel, J.K., Nuzzo, R.G., Whitesides, G.M.: Self-assembled monolayers of thiolates on metals as a form of nanotechnology. Chem. Rev. **105**, 1103–1169 (2005)
22. Lv, Z., Wang, J., Deng, L., Chen, G.: Preparation and characterization of covalent binding of rat anti-human IgG monolayer on thiol-modified gold surface. Nanoscale Res. Lett. **4**, 1403–1408 (2009)
23. Wakayama, J., Sekiguchi, H., Akanuma, S., Ohtani, T., Sugiyama, S.: Methods for reducing nonspecific interaction in antibody–antigen assay via atomic force microscopy. Anal. Biochem. **380**, 51–58 (2008)
24. Luthi, R., Meyer, E., Haefke, H., Howald, L., Gutmannsbauer, W., Guggisberg, M., Bammerlin, M., Guntherodt, H.J.: Nanotribology: an UHV-SFM study on thin films of C60 and AgBr. Surf. Sci. **338**, 247–260 (1995)
25. Nonnenmacher, M., Greschner, J., Wolter, O., Kassing, R.: Scanning force microscopy with micromachined silicon sensors. J. Vac. Sci. Technol. **B9**, 1358–1362 (1991)
26. Sader, J.E., Sader, R.C.: Susceptibility of atomic force microscope cantilevers to lateral forces: experimental verification. Appl. Phys. Lett. **83**, 3195–3197 (2003)
27. Sadaie, M., Nishikawa, N., Ohnishi, S., Tamada, K., Yase, K., Hara, M.: Studies of human hair by friction force microscopy with the hair-model-probe. Colloids Surf. B, Biointerfaces **51**, 120–129 (2006)
28. Lv, Z., Wang, J., Chen, G., Deng, L.: Probing specific interaction forces between human IgG and rat anti-human IgG by self-assembled monolayer and atomic force microscopy. Nanoscale Res. Lett. **5**, 1032–1038 (2010)
29. Chen, L.W., Cheung, C.L., Ashby, P.D., Lieber, C.M.: Single-walled carbon nanotube AFM probes: optimal imaging resolution of nanoclusters and biomolecules in ambient and fluid environments. Nano Lett. **4**, 1725–1731 (2004)
30. Clear, S.C., Nealey, P.F.: Chemical force microscopy study of adhesion and friction between surfaces functionalized with self-assembled monolayers and immersed in solvents. J. Colloid Interface Sci. **213**, 238–250 (1999)
31. Derjaguin, B.V., Muller, V.M., Toporov, Yu.P.: Effect of contact deformations on the adhesion of particles. J. Colloid Interface Sci. **53**, 314–326 (1975)
32. Johnson, K.L., Kendall, K., Roberts, A.D.: Surface energy and the contact of elastic solids. Proc. R. Soc. Lond., A. **324**, 301–313 (1971)
33. Berman, A., Drummond, C., Israelachvili, J.: Amontons' law at the molecular level. Tribol. Lett. **4**, 95–101 (1998)
34. Xiao, X., Hu, J., Charych, D.H., Salmeron, M.: Chain length dependence of the frictional properties of alkylsilane molecules self-assembled on mica studied by atomic force microscopy. Langmuir **12**, 235–237 (1996)
35. Kiely, J.D., Houston, J.E.: Contact hysteresis and friction of alkanethiol self-assembled monolayers on gold. Langmuir **15**, 4513–4519 (1999)
36. Brewer, N.J., Beake, B.D., Leggett, G.J.: Friction force microscopy of self-assembled monolayers: influence of adsorbate alkyl chain length, terminal group chemistry and scan velocity. Langmuir **17**, 1970–1974 (2001)
37. Gnecco, E., Bennewitz, R., Gyalog, T., Loppacher, Ch., Bammerlin, M., Meyer, E., Guntherodt, H.J.: Velocity dependence of atomic friction. Phys. Rev. Lett. **84**, 1172–1175 (2000)
38. Gnecco, E., Meyer, E.: Fundamentals of Friction and Wear, 1st edn. Springer, New York (2007)